

Time-Resolved Resonance Raman Evidence for Tight Coupling between Electron Transfer and Proton Pumping of Cytochrome *c* Oxidase upon the Change from the Fe^V Oxidation Level to the Fe^{IV} Oxidation Level

Takashi Ogura,^{†,‡} Shun Hirota,[‡] Denis A. Proshlyakov,[‡] Kyoko Shinzawa-Itoh,[§] Shinya Yoshikawa,[§] and Teizo Kitagawa^{*,†,‡}

Contribution from the Institute for Molecular Science, Okazaki National Research Institutes and The Graduate University for Advanced Studies, Myodaiji, Okazaki, 444 Japan, and Department of Life Science, Himeji Institute of Technology, Kamigori-cho, Ako-gun, Hyogo 678-02, Japan

Received June 12, 1995[⊗]

Abstract: The mechanism of dioxygen reduction catalyzed by cytochrome *c* oxidase, the terminal enzyme of the respiration chain of aerobic organisms, has been investigated with time-resolved resonance Raman spectroscopy. Five oxygen isotope sensitive Raman bands have been identified for ¹⁶O₂/¹⁸O₂ intermediates at 571/544, 804/764, 356/342, 785/750, and 450/425 cm⁻¹ in the order of appearance. The first and last ones, which have been assigned to the Fe^{III}-O₂⁻ and Fe^{III}-OH⁻ stretching modes, respectively, are in general consensus, but the remaining three bands are currently under debate. This study establishes that the 804/764 cm⁻¹ species is generated prior to the 785/750 cm⁻¹ species, and the latter is not observed when we start from the mixed valence enzyme. Therefore, the enzyme oxidation state of the 804/764 cm⁻¹ species is higher by one oxidative equivalent than that of the 785/750 cm⁻¹ species, although both bands have been assigned to the Fe=O stretching mode. The excitation wavelength dependences of these two sets of Raman bands are distinctly different, suggesting that the electronic properties of the two hemes are quite different. We found that the conversion from the 804/764 cm⁻¹ species to the 785/750 cm⁻¹ species was significantly slower in D₂O than in H₂O, suggesting strong coupling between electron and vector proton transfers at this stage. Presumably, Cu_B at the binuclear site causes heterolytic cleavage of the O—O bond, giving rise to an oxoiron in the Fe^V oxidation level of the enzyme with the 804/764 cm⁻¹ bands, and the electron transfer to this oxoiron is accompanied by some protein conformational changes, which cause distortion of the oxoheme and thus appearance of the His—Fe=O bending Raman bands at 356/342 cm⁻¹ and simultaneously active transport of protons.

Cytochrome *c* oxidase [E.C. 1.9.3.1] (CcO), the terminal enzyme in the mitochondrial electron transfer chain, catalyzes the reduction of dioxygen to water, which is coupled with vectorial proton translocation across the inner membrane.¹ Recently X-ray crystallographic structures have been solved for mammalian and bacterial cytochrome *c* oxidases.^{2,3} CcO has two heme A groups (Fe_a and Fe_{a3}) and two copper centers (Cu_A and Cu_B) as redox active metal centers. It is known that the Fe_{a3}-Cu_B binuclear center with 4.5 Å separation² serves as a catalytic site for dioxygen reduction, while the Fe_a and Cu_A centers receive electrons from cytochrome *c* and transfer them to the catalytic site. Extensive efforts have been made to elucidate a reaction mechanism of this enzyme, using time-resolved absorption,^{4–8} cryogenic absorption,^{9,10} EPR,^{11,12} and resonance Raman (RR) spectroscopy.^{13–15}

Time-resolved RR spectroscopy is uniquely powerful for elucidation of the reaction mechanism of CcO, since only this technique is able to detect the vibrations of dioxygen and its reductive intermediates bound to the catalytic site during the enzymatic turnover. Indeed, this technique has explored structures of reaction intermediates of various heme proteins.¹⁶ For cytochrome *c* oxidase, five oxygen isotope sensitive Raman bands have been identified at 571, 804, 356, 785, and 450 cm⁻¹. The first band was assigned to the Fe^{III}-O₂⁻ stretching mode,^{13–15} and the last band was assigned to the Fe^{III}-OH⁻ stretching mode.^{17,18} These are in general consensus, but the

(7) Oliveberg, M.; Brzezinski, P.; Malmstrom, B. G. *Biochim. Biophys. Acta* **1989**, *977*, 322–328.

(8) Verkховsky, M. I.; Morgan, J. E.; Wikstrom, M. *Biochemistry* **1994**, *33*, 3079–3086.

(9) Chance, B.; Saronio, C.; Leigh, J. S., Jr. *J. Biol. Chem.* **1975**, *250*, 9226–9237.

(10) Clore, G. M.; Andreasson, L. E.; Karlsson, B.; Aasa, R.; Malmstrom, B. G. *Biochem. J.* **1980**, *185*, 139–154.

(11) Hansson, O.; Karlsson, B.; Aasa, R.; Vanngard, T.; Malmstrom, B. G. *EMBO J.* **1982**, *1*, 1295–1297.

(12) Witt, S. N.; Chan, S. I. *J. Biol. Chem.* **1987**, *262*, 1446–1448.

(13) Han, S.; Ching, Y. -c.; Rousseau, D. L. *Proc. Natl. Acad. Sci. U.S.A.* **1990**, *87*, 8408–8412.

(14) Varotsis, C.; Woodruff, W. H.; Babcock, G. T. *J. Am. Chem. Soc.* **1989**, *111*, 6439–6440; **1990**, *112*, 1297.

(15) Ogura, T.; Takahashi, S.; Shinzawa-Itoh, K.; Yoshikawa, S.; Kitagawa, T. *J. Am. Chem. Soc.* **1990**, *112*, 5630–5631.

(16) Kitagawa, T.; Ogura, T. In *Advances in Spectroscopy*; Clark, R. J. H., Hester, R. E., Eds.; John Wiley & Sons: Chichester, 1993; Vol. 21, pp 139–188.

(17) Han, S.; Ching, Y. -c.; Rousseau, D. L. *Nature* **1990**, *348*, 89–90.

* To whom correspondence should be addressed.

† Ozaki National Research Institutes.

‡ Graduate University for Advanced Studies.

§ Himeji Institute of Technology.

⊗ Abstract published in *Advance ACS Abstracts*, June 1, 1996.

(1) Babcock, G. T.; Wikstrom, M. *Nature* **1992**, *356*, 301–309.

(2) Tsukihara, T.; Aoyama, H.; Yamashita, E.; Tomizaki, T.; Yamaguchi, H.; Shinzawa-Itoh, K.; Nakashima, R.; Yaono, R.; Yoshikawa, S. *Science* **1995**, *269*, 1069–1074.

(3) Iwata, S.; Ostermeier, C.; Ludwig, B.; Michel, H. *Nature* **1995**, *376*, 660–669.

(4) Gibson, Q. H.; Greenwood, C. *Biochem. J.* **1963**, *86*, 541–554.

(5) Orii, Y. *Ann. N. Y. Acad. Sci.* **1988**, *550*, 105–117.

(6) Hill, B. C.; Greenwood, C.; Nichols, P. *Biochim. Biophys. Acta* **1986**, *853*, 91–113.

remaining three bands are currently under debate with respect to both the order of appearance and the assignments. Establishing the order of appearance of the oxygen isotope sensitive bands is essential to elucidating the reaction mechanism of CcO, and for this purpose the present study was undertaken. We succeeded by lowering the temperature and also by extending the delay time. It was found that the 804 cm^{-1} species is higher in the oxidation state of the enzyme than the 785 cm^{-1} species and also that the intramolecular electron transfer to the 804 cm^{-1} species is significantly slower in D_2O than in H_2O , suggesting tight coupling of the electron transfer with translocation of vector protons at this stage. Structural implications of those Raman bands are discussed.

Materials and Methods

CcO was isolated from bovine heart muscle according to the method using cholate and Brij 35 as detergents,¹⁹ and dissolved in 50 mM sodium phosphate buffer, pH 7.2. The enzyme solution (ca. $500\text{ }\mu\text{M}$ in terms of heme A) was kept on ice until use and was always used within 10 days after isolation. About 80 mL of CcO solution ($50\text{ }\mu\text{M}$ CcO, $50\text{ }\mu\text{M}$ cytochrome *c*, 100 mM ascorbate, 20% ethylene glycol,²⁰ 50 mM sodium phosphate buffer, pH 7.2, no additional detergent) was subjected to an artificial cardiovascular system²¹ with further improvements on the lungs;²² the lungs for oxygen were replaced by those of a water-jacketed type to which temperature-controlled water ($-9\text{ }^\circ\text{C}$) containing 20% (v/v) ethylene glycol was circulated. The pump and probe wavelengths were 590 and 423 nm, respectively. The dead volume between the lung and the Raman cell was 3.6 mL. Since the flow rate was maintained at 40 mL/min, carbonmonoxy-CcO that has passed through the lung was exposed to O_2 for 5.4 s until the reaction was initiated by illumination of the pump laser beam, and during this period the temperature of the solution was raised from -9 to $+3\text{ }^\circ\text{C}$.

The dissociation rate constant of CO was reported to be 0.023 s^{-1} at $20\text{ }^\circ\text{C}$, pH 7.4, and becomes smaller at lower temperatures.⁹ We can estimate the population of CO-bound CcO at the Raman cell to be $e^{-0.023 \times 5.4} = 0.88$ at $20\text{ }^\circ\text{C}$. This means that, while the enzyme flows from the lung to the Raman cell, spontaneous replacement of CO by O_2 takes place by 12% at $20\text{ }^\circ\text{C}$. Since the present experiments were performed at much lower temperatures, the percentage of spontaneous replacement should be significantly smaller than 12%. This was confirmed by the preliminary observation that the spectra obtained without the pump light (probe-only spectrum) in the presence and absence of O_2 were virtually identical and exhibited the spectrum of the CO-bound form. Accordingly, spontaneous replacement of CO with O_2 before the exposure to pump light for initiating the reaction was negligible under the experimental conditions adopted here.

Results

Figure 1 shows the time-resolved RR difference spectra of CcO ($^{16}\text{O}_2$ derivative minus $^{18}\text{O}_2$ derivatives) for its reaction intermediates in H_2O at a certain delay time (Δt) between 0.1 and 5.4 ms after the initiation of the reaction. It was demonstrated previously²² that the difference peaks at $571/544\text{ cm}^{-1}$ for $^{16}\text{O}_2/^{18}\text{O}_2$ in spectrum A arose from the dioxygen adduct with end-on geometry. We pointed out the presence of two sets of difference patterns around 800 cm^{-1} for the subsequent intermediates,²² although they have not been resolved

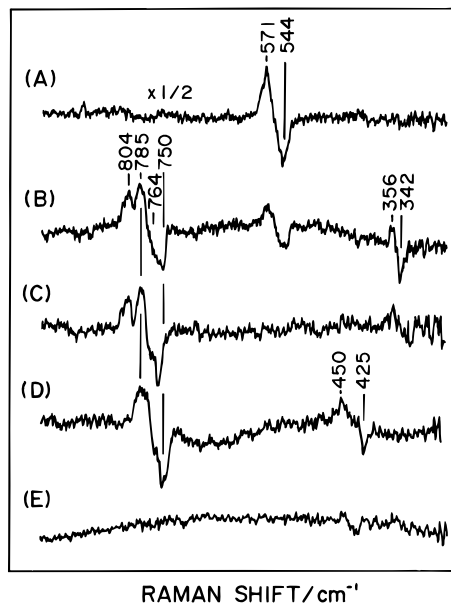


Figure 1. Time-resolved resonance Raman difference spectra of reaction intermediates of cytochrome *c* oxidase in H_2O . The Raman difference spectra obtained by subtracting the spectrum of the corresponding $^{18}\text{O}_2$ derivative from the spectrum of the $^{16}\text{O}_2$ derivative at each delay time are depicted. Therefore, positive and negative peaks denote the contributions of $^{16}\text{O}_2$ and $^{18}\text{O}_2$ derivatives, respectively. The delay time after initiation of the reaction is 0.1 (A), 0.27 (B), 0.54 (C), 2.7 (D), and 5.4 (E) ms. Excitation wavelength 423 nm. Temperature $3\text{ }^\circ\text{C}$.

in studies of other groups.^{17,23} Here we confirm the presence of two bands at $804/764$ and $785/750\text{ cm}^{-1}$ together with the low-frequency bands at $356/342\text{ cm}^{-1}$ in spectra B ($\Delta t = 0.27$ ms) and C ($\Delta t = 0.54$ ms).

The order of their appearance is much clearer in Figure 1 than in our previous study.²² Spectrum D, which exhibits only the $785/750\text{ cm}^{-1}$ pair near 800 cm^{-1} , strongly suggests that the $804/764\text{ cm}^{-1}$ pair precedes the $785/750\text{ cm}^{-1}$ pair, similar to that for the reaction of oxidized CcO with H_2O_2 .²⁴ The $450/425\text{ cm}^{-1}$ pair, which arises from the final species with the $\text{Fe}^{\text{III}}\text{-OH}$ heme^{17,18} at $\Delta t = 2.7$ ms (spectrum D), disappears at $\Delta t = 5.4$ ms (spectrum E) due to exchange of the bound hydroxyl anion with bulk water. The relative intensities of the $804/764\text{ cm}^{-1}$ bands to the $356/342\text{ cm}^{-1}$ bands were varied in repeated experiments, suggesting that these pairs arise from separate molecular species.

Figure 2 depicts similar difference spectra observed for the D_2O solution. Spectrum A ($\Delta t = 0.1$ ms) gives the $\text{Fe}^{\text{III}}\text{-O}_2^-$ stretching mode at $571/544\text{ cm}^{-1}$, being the same as that in Figure 1A. For delay times of $\Delta t = 0.54$ (B) and 2.7 ms (C), however, a single band was observed around 800 cm^{-1} (at $804/764\text{ cm}^{-1}$), contrary to the case for H_2O . Therefore, we previously described²² that the $785/750\text{ cm}^{-1}$ pair in the H_2O solution was shifted to $796/766\text{ cm}^{-1}$ in D_2O , giving rise to an overlapping band centered around 800 cm^{-1} . However, it turned out from this experiment that the lifetime of the $804/764\text{ cm}^{-1}$ species is so different in H_2O and D_2O that the $785/750\text{ cm}^{-1}$ species was not generated in D_2O at $\Delta t = 2.7$ ms when it was generated in H_2O . It is noted that the $356/342\text{ cm}^{-1}$ bands are clearly seen in spectra B and C at the same frequencies as those in the H_2O solution.

Spectra D ($\Delta t = 6.5$ ms) and E ($\Delta t = 11$ ms) for the D_2O solution demonstrated that the $785/750\text{ cm}^{-1}$ bands did appear

(18) Ogura, T.; Takahashi, S.; Shinzawa-Itoh, K.; Yoshikawa, S.; Kitagawa, T. *Bull. Chem. Soc. Jpn.* **1991**, *64*, 2901–2907.

(19) Yoshikawa, S.; Choc, M. G.; O'Toole, M. C.; Caughey, W. S. *J. Biol. Chem.* **1977**, *252*, 5498–5508.

(20) Ethylene glycol was omitted for measurements of Figures 3 and 4 conducted at 0 and $5\text{ }^\circ\text{C}$, respectively.

(21) Ogura, T.; Yoshikawa, S.; Kitagawa, T. *Biochemistry* **1989**, *28*, 8022–8027.

(22) Ogura, T.; Takahashi, S.; Hirota, S.; Shinzawa-Itoh, K.; Yoshikawa, S.; Appelman, E. H.; Kitagawa, T. *J. Am. Chem. Soc.* **1993**, *115*, 8527–8536.

(23) Varotsis, C.; Zhang, Y.; Appelman, E. H.; Babcock, G. T. *Proc. Natl. Acad. Sci. U.S.A.* **1993**, *90*, 237–241.

(24) Proshlyakov, D. A.; Ogura, T.; Shinzawa-Itoh, K.; Yoshikawa, S.; Kitagawa, T. *Biochemistry* **1996**, *35*, 76–82.

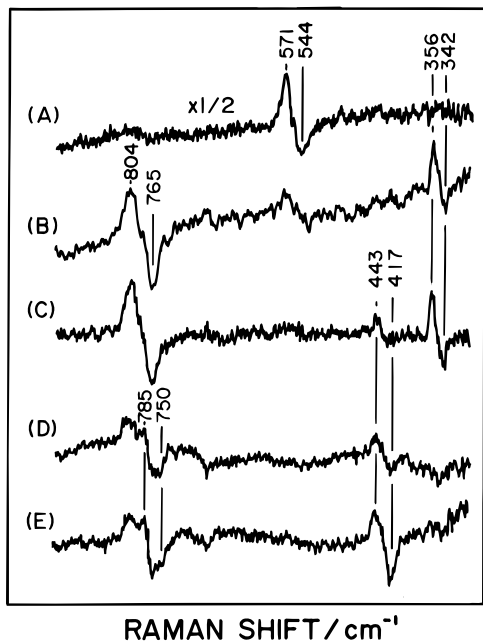


Figure 2. Time-resolved resonance Raman difference spectra of reaction intermediates of cytochrome *c* oxidase in D₂O. The delay time is 0.1 (A), 0.54 (B), 2.7 (C), 6.5 (D), and 11 (E) ms. Other conditions are the same as those for Figure 1.

at the same frequency but much later than in the case of H₂O solution. This means that the conversion from the 804/764 cm⁻¹ species to the 785/750 cm⁻¹ species occurs in D₂O similar to the H₂O solution but its rate is significantly slow in D₂O compared with that in H₂O. This is consistent with the fact that the corresponding rate in D₂O is found to be one-fifth of that in H₂O for the peroxide reaction.²⁵ The subsequent appearance of the 443/417 cm⁻¹ bands, which arise from the Fe^{III}-OD stretching, is consistent with the results shown in Figure 1. The experiments for $\Delta t = 0.3$ – 0.5 ms for D₂O solutions (data not shown) yielded the 804/764 and 356/342 cm⁻¹ bands in a manner similar to that of spectrum B. Although Varotsis *et al.* suggested²³ that the 356 cm⁻¹ band preceded the 790 cm⁻¹ band in their spectra, it is not clear whether the 356 cm⁻¹ band precedes the 804 cm⁻¹ band, since they failed to observe the 804 cm⁻¹ band.

The facts that the frequency of the 785/750 cm⁻¹ bands remained unchanged in D₂O and that the 804/764 cm⁻¹ species appeared prior to the 785/750 cm⁻¹ species forced us to retract our previous assignments²² of them to the Fe^{IV}=O and Fe^{III}OOH species. When the mixed valence CO-bound enzyme, which had only two electrons in a molecule, was used as a starting material instead of the fully reduced CO-bound enzyme, which had four electrons, we observed the Fe-O₂ intermediate with bands at 571/544 cm⁻¹ as the primary intermediate followed by appearance of the bands at 804/764 and 356/342 cm⁻¹ (data not shown). These bands lasted as long as $\Delta t = 4.2$ ms, but the bands at 785/750 and 450/425 cm⁻¹ did not appear in this case. These results definitely indicate that the species giving rise to the 804/764 cm⁻¹ pair has the oxidation state higher than that of the 785/750 cm⁻¹ species.

In this study the sample-flowing dual-beam technique using two CW lasers^{26–28} was adopted instead of two pulsed lasers

(25) Proshlyakov, D. A.; Ogura, T.; Shinzawa-Itoh, K.; Yoshikawa, S.; Kitagawa, T. *Biochemistry*, in press.

(26) Smith, S. O.; Pardo, J. A.; Mulder, P. P. J.; Curry, B.; Lugtenburg, J.; Mathies, R. A. *Biochemistry* **1983**, *22*, 6141–6148.

(27) Ogura, T.; Maeda, A.; Nakagawa, M.; Kitagawa, T. In *Primary Processes in Photobiology*, Kobayashi, T., Ed.; Springer: New York, 1987; Vol. 20, pp 233–241.

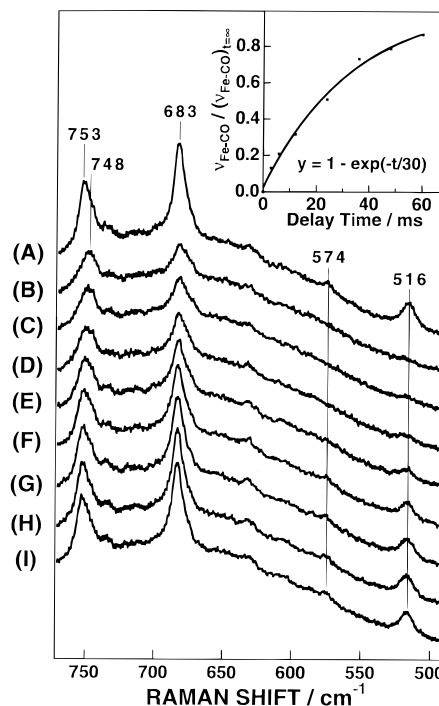


Figure 3. Time-resolved resonance Raman spectra for photodissociation and recombination processes of CO-bound fully reduced cytochrome *c* oxidase. The delay time of individual spectra is (A) -12 , (B) 0.6, (C) 3, (D) 6, (E) 12, (F) 24, (G) 36, (H) 48, and (I) 60 ms. The inset plots the intensities of the 516 cm⁻¹ bands of individual spectra relative to that of spectrum A against delay times, and thus represents the time profile of the population of recombined CcO. The solid line indicates a theoretical curve fitted to the experimental points with $y = 1 - \exp(-t/30)$. Temperature 0 °C.

for time-resolved Raman measurements. The 356/342 cm⁻¹ pair were observed around $\Delta t = 0.3$ – 1.0 ms in this experiment but only at 0.16 ms in the measurements with pulsed lasers.²³ It is important to check the accuracy in the time axis of the present experiment. The time resolution and accuracy in this experiment depend upon several factors including the flow rate, stability of the peristaltic pump, uniformity of the sample flow in a Raman cell, and width of the laser beams. To clarify the practical situation under the present experimental conditions, we examined time-resolved RR spectra for carbonmonoxy-CcO in the absence of oxygen.

Figure 3 shows the results. Temporal changes of spectra seen in Figure 3 reflect photodissociation and recombination of CO at the Fe_{a3} site. Spectrum A with $\Delta t = -12$ ms corresponds to the probe-only spectrum and accordingly exhibits the spectrum of CO-bound CcO. The band at 516 cm⁻¹ is due to the Fe-CO stretching ($\nu_{\text{Fe-CO}}$) vibration.^{29,30} In spectrum B with $\Delta t = 0.6$ ms the band at 516 cm⁻¹ is absent, indicating complete photodissociation of CO. It is evident that the band intensity at 516 cm⁻¹ is gradually restored as going from spectrum C with $\Delta t = 3$ ms to spectrum I with $\Delta t = 60$ ms.

The inset of Figure 3 plots the intensities of the $\nu_{\text{Fe-CO}}$ RR bands at given Δt relative to that at $\Delta t = -12$ ms against the delay time, and accordingly, the ordinate (*y*) stands for a fraction of CO-recombined CcO. The solid line denotes the least squares fit by the function $y = 1 - \exp(-kt)$, to the observed data on the assumption that this process is modeled by the first-order

(28) Han, S.; Ching, Y. -c.; Rousseau, D. L. *J. Am. Chem. Soc.* **1990**, *112*, 9445–9451.

(29) Argade, P. V.; Ching, Y. -c.; Rousseau, D. L. *Science* **1984**, *225*, 329–331.

(30) Hirota, S.; Ogura, T.; Shinzawa-Itoh, K.; Yoshikawa, S.; Nagai, M.; Kitagawa, T. *J. Phys. Chem.* **1994**, *98*, 6652–6660.

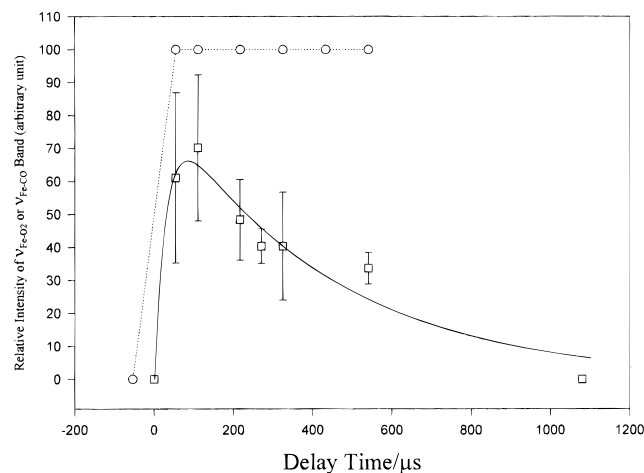


Figure 4. Temporal profile of the Fe–O₂ intermediate evaluated with the $\nu_{\text{Fe-O}_2}$ Raman bands at 571/544 cm^{-1} for $^{16}\text{O}_2/^{18}\text{O}_2$. Open squares indicate the valley to peak height of the 571/544 cm^{-1} bands in individual spectra relative to the peak height of the ν_7 band in the corresponding raw spectrum. The solid line shows a least-squares fitting to the data points assuming $y = A_0[1 - \exp(-k_1t)] \exp(-k_2t)$. The k_1 and k_2 thus estimated are 3.2×10^4 and $2.4 \times 10^3 \text{ s}^{-1}$, respectively. Open circles plot the fractional population of CO-photodissociated CcO obtained under the same experimental conditions except for the absence of O₂, while the broken line is drawn for easy viewing. The values in the ordinate denote the fraction of the CO-dissociated form and have no relation with the curve for the population of the dioxy intermediate. Temperature 5 °C.

reaction kinetics. The numerical fitting yielded $k = 33 \text{ s}^{-1}$. The association rate constant of CO to CcO was reported to be about $3.5 \times 10^4 \text{ M}^{-1} \text{ s}^{-1}$ at 0 °C.³¹ Since the concentration of CO was approximately $1 \times 10^{-3} \text{ M}$ in this experiment (equilibrium with the partial pressure of 1 atm), the first-order association rate is calculated to be 35 s^{-1} . The value obtained here (33 s^{-1}) is in remarkably good agreement with it. Consequently, the dual-beam flow apparatus used here has been proved to show correct numbers of delay time in the region of several tens of milliseconds.

In order to check the apparatus for the short delay time region, we carried out the same experiments as those in Figure 3 in the delay time region shorter than 1 ms. Figure 4 depicts the plot of the valley to peak height of the $\nu_{\text{Fe-O}_2}$ Raman band at 571 cm^{-1} (open squares) relative to the peak height of the ν_7 band at 683 cm^{-1} in the raw spectra against delay times. The ordinate stands for the population of the Fe–O₂ intermediate. The time profile of the CO-photodissociated reduced species, obtained from the intensity of the $\nu_{\text{Fe-CO}}$ band at 516 cm^{-1} in the absence of O₂, is also plotted and represented by open circles in Figure 4. The difference between those two measurements lies in whether O₂ was present or not, but otherwise the experimental conditions were exactly the same. In other words, open squares in Figure 4 represent the practical rise and decay curves of the primary dioxy intermediate in the present experimental conditions. We failed to obtain the spectrum for $\Delta t = 0 \mu\text{s}$ due to interference from the spatially overlapped pump beam.

Discussion

Accuracy of Delay Times. In the analysis of the results shown in Figure 4, we assumed that the photodissociation was complete at $\Delta t = 0 \mu\text{s}$ but that the concentration of the Fe–O₂ intermediate at $\Delta t = 0 \mu\text{s}$ was zero. Then, the concentration (y) of the Fe–O₂ species at a given time can be approximated

by $y = [1 - \exp(-k_1t)] \exp(-k_2t)$. Numerical fitting yielded the rise (k_1) and decay (k_2) rate constants of the Fe–O₂ intermediate to be 3.2×10^4 and $2.4 \times 10^3 \text{ s}^{-1}$, respectively. The rise rate constant is in practical agreement with that reported by Blackmore *et al.* ($3.5 \times 10^4 \text{ s}^{-1}$).³² Since this process involves movements of O₂ from Cu_B to Fe_{a3}, a process with a small activation energy, the rate would only be slightly affected by the temperature change from 23 to 5 °C. The decay rate constant would also be consistent with their value of $1.0 \times 10^4 \text{ s}^{-1}$, if we take the temperature difference into consideration; if the activation energy for the reaction is assumed to be 10 kcal/mol ($4.2 \times 10^4 \text{ J}\cdot\text{mol}^{-1}$), the ratio of reaction rates at 23 and 5 °C is 3.0. This means that if the present experiment were performed at 23 °C, the decay rate of the dioxygen complex would be $2.4 \times 10^3 \times 3.0 = 7.2 \times 10^3 \text{ s}^{-1}$. This number is also comparable to one other reported value,³³ but differs from others.^{8,34,35} One of the reasons for the discrepancy is whether one regards the first phase of the absorbance change as the binding of O₂ to Cu_B or to Fe_{a3}. In addition, there are other factors which may affect the apparent rate constants: temperature, the concentration of O₂, the concentration and nature of the detergent, and so on. Although the origin of the discrepancy in rate constants remains to be clarified in the future, we stress that the rise and decay rates of the Fe–O₂ intermediate are compatible to a group of reported data.

The sample flow in this kind of experiment should be a laminal flow instead of a turbulent flow in the cell. This can be checked with the Reynolds number, $Re = v*d/\zeta$, where v , d , and ζ denote the average velocity of the fluid [ms^{-1}], inner diameter of the tube [m] (here a round tube is assumed), and kinematic viscosity [$\text{m}^2 \text{ s}^{-1}$]. Since the kinematic viscosity of water at 0 °C is 1.8×10^{-6} and it is larger for the ethylene glycol solution, the upper limit of the Reynolds number for the present system is calculated to be $Re = 1.9 \text{ ms}^{-1} \times 0.6 \times 10^{-3} \text{ m} / 1.8 \times 10^{-6} \text{ m}^2 \text{ s}^{-1} = 633$ for a 0.6 mm \times 0.6 mm cell and a flow rate of 40 mL/min. According to fluid mechanics, a flow is laminal when the Reynolds number is less than 2300. Therefore, it is clear that the flow in the Raman cell is a laminal flow but is not a turbulent flow under the experimental conditions adopted in this study.

Assignment of the Bands at 804 and 785 cm^{-1} . In the steady-state experiments for the reaction of oxidized CcO with H₂¹⁶O₂/H₂¹⁸O₂, three oxygen isotope sensitive bands were observed at 804/764, 356/342, and 785/750 cm^{-1} upon blue excitation.²⁴ The 785/750 cm^{-1} bands could not be recognized upon excitation at 607 and 580 nm³⁶ under the conditions where those bands are known to exist. Upon excitation at 607 nm for the same reaction, however, the 804/764 cm^{-1} pair were identified when the “607 nm” absorption form existed,³⁶ which is the primary intermediate in the reaction of oxidized CcO with H₂O₂. Although the “607 nm” form is called a “peroxy” intermediate, the oxoiron structure of the heme for this form was demonstrated by asymmetric isotope substitution experiments using H₂¹⁶O¹⁸O.³⁶

On the other hand, it was previously demonstrated for dioxygen reduction using ¹⁶O¹⁸O that the 804/765 cm^{-1} intermediate also has an oxoheme.²² This intermediate was also

(32) Blackmore, R. S.; Greenwood, C.; Gibson, Q. H. *J. Biol. Chem.* **1991**, *266*, 19245–19249.

(33) Oliveberg, M.; Malmstrom, B. G. *Biochemistry* **1992**, *31*, 3560–3563.

(34) Han, S.; Ching, Y. -c.; Rousseau, D. L. *Proc. Natl. Acad. Sci. U.S.A.* **1990**, *87*, 2491–2495.

(35) Orii, Y. *Chem. Scr.* **1988**, *28A*, 63–69.

(36) Proshlyakov, D. A.; Ogura, T.; Shinzawa-Itoh, K.; Yoshikawa, S.; Appelman, E. H.; Kitagawa, T. *J. Biol. Chem.* **1994**, *269*, 29385–29388.

(31) A value derived from Figure 2 in ref 4.

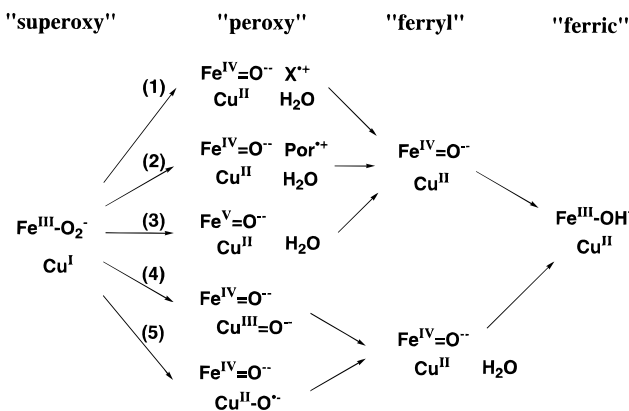


Figure 5. Possible pathways for reduction of O₂ bound to the binuclear center of cytochrome *c* oxidase. "Peroxy" and "ferryl" mean the Fe^V and Fe^{IV} oxidation levels of the enzyme, respectively. "Por", "Por^{•+}", and "X^{•+}" mean neutral porphyrin, its π cation radical, and an amino acid cation radical, respectively. See the text for details.

detected upon excitation at 607 nm,³⁷ but the 784/750 cm⁻¹ bands could not be recognized upon excitation at 607 and 441.6 nm for the dioxygen reaction.³⁷ The frequency and the size of the isotopic frequency shift of the 785/750 cm⁻¹ bands make it quite reasonable to assign the band to the ferryl-oxo compound like compound II of HRP.³⁸

These results mean that similar intermediates are generated in the dioxygen and peroxide reactions and that the heme electronic properties of the 804/764 cm⁻¹ and 784/750 species are dissimilar. It became evident that the 804/764 cm⁻¹ species has a higher oxidation state than the 785/750 cm⁻¹ species and thus belongs to the Fe^V (or so-called peroxy) oxidation level of the enzyme.

Pathway of O₂ Reduction by CcO. Figure 5 illustrates possible reaction pathways for dioxygen reduction by CcO. The first (Fe^{III}-O₂⁻) and the last (Fe^{III}-OH⁻) intermediates have already been established. There is no doubt about the formation of neutral Fe_{a3}^{IV}=O heme in the three electron reduced state, irrespective of pathways 1–5 in Figure 5. This corresponds to the "580 nm" form in the reaction of oxidized CcO with H₂O₂ in agreement with the frequencies of oxygen isotope sensitive RR bands of this complex.²⁵ A possible Fe^V oxidation level of heme proteins has so far been practically seen in the upper two cases (1 and 2):³⁸ (1) an Fe^{IV}=O porphyrin with an amino acid radical (X^{•+}) like compound ES of cytochrome *c* peroxidase (CcP) and (2) an Fe^{IV}=O porphyrin π cation radical like compound I of horseradish peroxidase. There are at least three other possibilities in the case of CcO: (3) an Fe^V=O porphyrin with d³ iron, (4) an Fe^{IV}=O porphyrin with Cu_B^{III}=O, and (5) an Fe^{IV}=O porphyrin with a Cu_B^{II}-O[•] oxygen radical. Reaction pathways 2 and 3 involve the heterolytic cleavage of the O–O bond, while pathways 4 and 5 correspond to homolysis. For pathway 1 the reaction can proceed through either heterolytic or homolytic cleavage.

For the so-called peroxy intermediate there have been no EPR data which exhibit the $g = 2$ signal arising from an amino acid radical. Therefore, there is no positive support for pathway 1. Furthermore, in this case the heme of the 804/764 cm⁻¹ species should exhibit properties of a Fe^{IV}=O porphyrin similar to those of the 785/750 cm⁻¹ species, which is contrary to the experimental facts mentioned above, and the putative amino acid radical should strongly interact with the Fe^{IV}=O bond so as to

raise its stretching frequency by 20 cm⁻¹ compared with the 785/750 cm⁻¹ species. These features are strongly unfavorable to this proposal. However, if an amino acid radical is generated near both the Fe^{IV}=O heme and the Cu_B^{II} ion, then the EPR signal may become extremely weak due to antiferromagnetic coupling and the Fe^{IV}=O bond may become stronger due to the cationic property of the radical (X^{•+}). Such a situation would only be consistent with pathway 1 from the experimental data currently available. In the case of pathway 2, porphyrin π cation radicals usually have significantly reduced Soret absorbance compared with neutral Fe^{IV}=O porphyrins. Since the Soret absorption of the 804/764 cm⁻¹ species is of ordinary intensity, the possibility that this species contains a porphyrin π cation radical may be ruled out.

When the homolytic cleavage of the O–O bond takes place immediately after instantaneous formation of the Fe^{III}-O⁻-O⁻-Cu_B^{II} structure, two oxometal centers, that is, Fe^{IV}=O heme and Cu_B^{III}=O will be generated [pathway 4 in Figure 5]. The Cu_B^{III}=O could be Cu_B^{II}-O[•] as assumed in pathway 5. In this case possible interactions between the Fe^{IV}=O and Cu_B^{III}=O (or Cu_B^{II}-O[•]) units would raise the $\nu_{\text{Fe=O}}$ frequency in the Fe^V oxidation level compared with the subsequent Fe^{IV}=O state and the 356/342 cm⁻¹ bands might arise from the Cu_B moiety. The trouble in this interpretation lies in that the 356/342 cm⁻¹ frequencies are too low to assign them to the Cu_B^{III}=O stretching mode and that the lifetime of the 356/342 cm⁻¹ species is too long to attribute it to an unstable Cu^{II}-O[•] radical species. Tolman and co-workers³⁹ recently observed the Cu^{III}=O (or Cu(OO)Cu in-phase) stretching mode at 606/583 cm⁻¹ upon homolysis of dicopper-¹⁶O₂/¹⁸O₂ complexes. The mechanism of resonance enhancement of the Cu_B^{III}=O stretching mode could be ascribed to a possible CT band in the blue region buried by the strong Soret band. Either in pathway 4 or in pathway 5, however, the hemes of the 804/764 and 785/750 cm⁻¹ species should have basically an identical excitation-wavelength dependence, contrary to the observed facts.

Feasibility of the Fe^V=O Heme. When one tries to oxidize an Fe^{IV}=O heme, it cannot be predicted *a priori* whether an electron is removed from the metal ion or from the porphyrin macrocycle. There are two electrons in the degenerate d_{xz} and d_{yz} orbitals of a low-spin Fe^{IV} ion, but it is not apparent whether the d_{xz} and d_{yz} orbitals are energetically higher than the highest occupied π orbitals of the porphyrin macrocycle with a_{1u} or a_{2u} symmetry or *vice versa*. When some electron-withdrawing substituents are attached to the porphyrin macrocycle, the a_{1u} or a_{2u} level is lowered⁴⁰ and may become lower than the iron d_{xz} and d_{yz} orbitals. Then an electron may be taken out of the iron orbital, generating an Fe^V state. Since the formyl substituent of heme A is strongly electron-withdrawing, generation of the Fe^V state is plausible. Furthermore, the d_{xz} and d_{yz} orbitals may serve as an antibonding orbital regarding the Fe=O π bond; it is reasonable that removal of this electron raises the Fe=O stretching frequency compared with that of the Fe^{IV}=O heme. In addition, the increase of a positive charge in the metal ion would strengthen the Fe^V=O bond compared with the Fe^{IV}=O bond.

The quite different excitation-wavelength dependences of the 804/764 and 785/750 cm⁻¹ RR bands would be understandable in this interpretation. This would also be consistent with the fact that similar time-resolved measurements on cytochrome *bo* with heme O at the O₂ binding site gave rise to the 788 cm⁻¹

(37) Matysik, J.; Ogura, T.; Shinzawa-Itoh, K.; Yoshikawa, S.; Kitagawa, T. To be published.

(38) Kitagawa, T.; Mizutani, Y. *Coord. Chem. Rev.* **1994**, *135*, 685–735.

(39) Mahapatra, S.; Halfen, J. A.; Wilkinson, E. C.; Pan, G.; Cramer, C. J.; Que, L. Jr.; Tolman, W. B. *J. Am. Chem. Soc.* **1995**, *117*, 8865–8866.

(40) Fujii, H.; Ichikawa, K. *Inorg. Chem.* **1992**, *31*, 1110–1112.

band but not the 804 cm^{-1} band in the transient states,⁴¹ if we consider that heme O lacks a strong electron-withdrawing group such as a formyl group.

One may argue against this proposal since the stretching force constant of $\text{Mn}^{\text{IV}}=\text{O}$ (4.15 $\text{mdyn}/\text{\AA}$) with a high-spin d^3 metal is smaller than that of $\text{Fe}^{\text{IV}}=\text{O}$ (5.20 $\text{mdyn}/\text{\AA}$) with a low-spin d^4 metal.⁴² There have been no data on the $\text{Fe}^{\text{V}}=\text{O}$ stretching mode for model porphyrin systems. However, the following analysis of data available does not justify the argument raised. The $\text{Mn}^{\text{V}}=\text{O}$ and $\text{Mn}^{\text{V}}=\text{N}$ stretching bands for the five-coordinate porphyrin complexes are reported at 979⁴³ and 1049 cm^{-1} ,⁴⁴ respectively. A simple diatomic harmonic approximation yields force constants of 7.00 and 7.24 $\text{mdyn}/\text{\AA}$ for the $\text{Mn}^{\text{V}}=\text{O}$ and $\text{Mn}^{\text{V}}=\text{N}$ bonds, respectively. The force constant of the $\text{Mn}^{\text{V}}=\text{O}$ bond is 3.3% smaller than that of the $\text{Mn}^{\text{V}}=\text{N}$ bond. The $\text{Fe}^{\text{V}}=\text{N}$ stretching band is reported at 876 cm^{-1} .⁴⁵ If the $\text{Fe}^{\text{V}}=\text{O}$ stretching force constant is assumed to be 96.7% of the $\text{Fe}^{\text{V}}=\text{N}$ stretching force constant (5.06 $\text{mdyn}/\text{\AA}$) similar to the Mn^{V} case, the $\text{Fe}^{\text{V}}=\text{O}$ stretching frequency would be calculated at 817 cm^{-1} for a five-coordinate complex. This frequency would be lowered by binding of a trans ligand,⁴⁶ and the stronger the trans ligand, the lower the $\text{Fe}^{\text{V}}=\text{O}$ stretching frequency. Since the proximal histidine remains bound at the trans position of the oxo oxygen in the protein during the reaction, the assignment of the 804 cm^{-1} band to the $\text{Fe}^{\text{V}}=\text{O}$ stretching of the six-coordinate heme appears reasonable.

In contrast with extensive studies on vibrational properties of the $\text{Fe}^{\text{IV}}=\text{O}$ hemes and $\text{Fe}^{\text{IV}}=\text{O}$ porphyrin π cation radicals,³⁸ those on $\text{Fe}^{\text{V}}=\text{O}$ heme are scarce. Therefore, the formation of $\text{Fe}^{\text{V}}=\text{O}$ heme as a reaction intermediate of an aa₃-type cytochrome *c* oxidase cannot be ruled definitive at the present time, but it is a most likely candidate.

Assignment of the 356/342 cm^{-1} Band. Ogura *et al.*¹⁸ reported the oxygen isotope sensitive band at 356 cm^{-1} (342 cm^{-1} for $^{18}\text{O}_2$) for the first time and assigned it to the $\text{Fe}-\text{OOH}$ stretching mode, because in that experiment they simultaneously observed a single oxygen isotope sensitive band around 790 cm^{-1} with a time profile similar to that of the 356 cm^{-1} band, as if both bands arose from an identical molecular species. At that stage they regarded the band around 790 cm^{-1} as the $\text{O}-\text{O}$ stretching vibration of the FeOOH unit.¹⁸ Both the $\text{Fe}^{\text{IV}}=\text{O}$ and O^--O^- stretching vibrations are expected to appear around 800 cm^{-1} , and they cannot be distinguished by the use of $^{16}\text{O}_2/^{18}\text{O}_2$. Furthermore, the ordinary $\text{Fe}^{\text{IV}}=\text{O}$ heme is expected to give rise to only one oxygen isotope sensitive Raman band, while the FeOOH heme could give more oxygen isotope sensitive bands including the $\text{Fe}-\text{OOH}$ stretching and $\text{Fe}-\text{O}-\text{O}$ bending and $\text{O}-\text{O}$ stretching vibrations.

Later, however, they retracted that proposal on the basis of new observations with a higher resolution spectrometer.²² The band around 800 cm^{-1} was resolved into two bands at 804 and 785 cm^{-1} . The 356/342 cm^{-1} bands could not be recognized upon 441.6 nm excitation, upon which the 804/764 cm^{-1} bands were clearly observed.³⁷ On the other hand, in the reaction of oxidized CcO with H_2O_2 , the 356/342 cm^{-1} bands were

observed together with the 785/750 cm^{-1} bands with complete absence of the 804/764 cm^{-1} bands.²⁵ These observations strongly suggest that the 356/342 cm^{-1} bands arise from a separate molecular species, which is consistent with the conclusion for dioxygen reaction²² in that the bands at 804, 785, and 356 cm^{-1} arise from different species. Varotsis and Babcock²³ observed the band at 356 cm^{-1} in their TR³ spectra in a time range between the appearance of bands at 571 and 790 cm^{-1} , and they thought that the 356 cm^{-1} band was due to an $\text{Fe}-\text{OOH}$ stretching vibration. However, since they failed to see the band at 804 cm^{-1} , it is not clear whether the 356 cm^{-1} band precedes the 804 cm^{-1} band or not. They reported that the band at 356 cm^{-1} was observable only at $\Delta t = 0.16$ ms, noting that the life time of the species in question was not long. However, we observed this band with delay times between 0.4 and 2.2 ms.¹⁸ This was recently confirmed by Takahashi and Rousseau⁴⁷ who observed the band with delay times between 0.13 and 0.98 ms.

In Figures 1 and 2, the time profiles of the 356/342 cm^{-1} bands seem to go in parallel with that of the bands at 804/786 cm^{-1} as if the species giving the 356 cm^{-1} band belonged to the peroxy oxidation level. On the contrary, the recent RR study on the reaction of oxidized CcO with H_2O_2 has shown that the species giving rise to the 356 cm^{-1} band belongs to the ferryl oxidation level rather than to the peroxy oxidation level.²⁵ In addition, the H_2O_2 experiments suggest that the 356 cm^{-1} species has another broad oxygen isotope sensitive band around 800 cm^{-1} , which is not clearly resolved in Figures 1 and 2 in this study for dioxygen reduction. Taking these features into consideration, we locate the 356/342 cm^{-1} species between the 804/764 and 785/750 cm^{-1} species in the reaction pathway.

It has been clarified²² from the $\text{H}_2\text{O}/\text{D}_2\text{O}$ insensitivity and $^{16}\text{O}/^{18}\text{O}$ frequency shifts that the 356/342 cm^{-1} bands should arise from a metal-oxo species. In the upright structure of the oxoheme with C_{4v} symmetry, the $\text{His}-\text{Fe}=\text{O}$ bending vibration is degenerate and Raman inactive in the absence of structural distortion. Since the $\text{Fe}^{\text{IV}}=\text{O}$ bond adopts an upright structure in the absence of special protein force, the $\text{His}-\text{Fe}^{\text{IV}}=\text{O}$ bending Raman band cannot be seen in compound II of various peroxidases. A likely interpretation of the 356/342 cm^{-1} bands is to assume that the $\text{Fe}=\text{O}$ bond is distorted from the ordinary upright structure and a $\text{His}-\text{Fe}=\text{O}$ bending vibration is allowed to appear. The distorted $\text{Fe}=\text{O}$ species is postulated to give the $\text{Fe}=\text{O}$ stretching mode near 800 cm^{-1} overlapped with the 804 cm^{-1} band. This distortion is caused presumably by protein structural forces coupled with the redox change of heme. It is highly desirable to examine Raman spectra of distorted model $\text{Fe}=\text{O}$ porphyrins to establish the assignment of this band. An alternative assignment is to ascribe it to the $\text{Cu}_B^{\text{II}}-\text{O}^\bullet$ radical species in pathway 5 as discussed above, but it is contradictory to the observations of this band for the 580 nm form in the peroxide reaction.²⁵

Coupling between Electron and Proton Transfers. RR studies on the peroxide reaction have demonstrated that the $\text{O}-\text{O}$ bond is already cleaved at the peroxy level.³⁶ This study has established that the change from the 804/764 cm^{-1} species to the 785/750 cm^{-1} species via the 356/342 cm^{-1} species is significantly slower in D_2O than in H_2O . This was also confirmed in recent studies of oxidized CcO with H_2O_2 .²⁵ Although the assignment of the 356/342 cm^{-1} bands is a key to interpretation of the reaction mechanism, we are tempted to propose pathway 3 in Figure 5 due to the reasons mentioned above. However, we cannot rule out a possibility that more than one pathway coexists in the enzymatic reaction and

(41) Hirota, S.; Mogi, T.; Ogura, T.; Hirano, T.; Anraku, Y.; Kitagawa, T. *FEBS Lett.* **1994**, *352*, 67–70.

(42) Czernuszewicz, R. S.; Su, Y. O.; Stern, M. K.; Macor, K. A.; Kim, D.; Groves, J. T.; Spiro, T. G. *J. Am. Chem. Soc.* **1988**, *110*, 4158–4165.

(43) Collins, T. J.; Powell, R. D.; Slobodnick, C.; Uffelman, E. S. *J. Am. Chem. Soc.* **1990**, *112*, 899–901.

(44) Champochiaro, C.; Hofmann, J. A.; Bocian, D. F. *Inorg. Chem.* **1985**, *24*, 449–450.

(45) Wagner, W.-D.; Nakamoto, K. *J. Am. Chem. Soc.* **1989**, *111*, 1590–1598.

(46) Su, Y. O.; Czernuszewicz, R. S.; Miller, L. A.; Spiro, T. G. *J. Am. Chem. Soc.* **1988**, *110*, 4150–4157.

(47) Takahashi, S.; Rousseau, D. L. Private communication.

branching occurs in the peroxy level. Accordingly, Babcock et al.⁴⁸ proposed the Fe—O—O—H structure in a branched pathway to assign their 356/342 cm⁻¹ species to the Fe—OOH stretching. The other possibility is to assign them to the Cu_B moiety. However, this frequency is too low to assign them to Cu^{III}=O stretching mode, and deuteration insensitivity²² prohibits us from assigning them to the Cu^{II}—OH stretching.

If our assignment is correct, it turns out that the conversion rate from the Fe^V oxidation level to the Fe^{IV}=O oxidation level is accompanied by distortion of the oxoheme due to some protein force. Since the conversion from the Fe^V=O heme to the Fe^{IV}=O heme itself does not need a proton, its rate would normally be similar in H₂O and D₂O. Presumably, scalar protons can come into and go out of the binuclear site without significant resistance and yield little difference in the reaction rate between H₂O and D₂O, as seen for the release of the first water molecule (that is, for the second electron transfer). The slower rate in D₂O in this step, in particular, suggests that this

(48) Varotsis, C. A.; Babcock, G. T. *J. Am. Chem. Soc.* **1995**, *117*, 11260–11269.

electron transfer is tightly coupled with the translocation of vector protons, which is against the gradient of proton concentrations and thus needs some energy. If this interpretation is correct, the redox energy is converted to electrochemical energy via some conformational change of protein as suggested before.⁴⁹ We stress that these results would open a new page in understanding the mechanism of dioxygen reduction by CcO and its coupling with proton pumping.

Acknowledgment. The authors would like to thank Professor R. Czernuszewicz of the University of Houston for his critical reading of this paper and stimulating discussion. The authors are grateful to Drs. S. Takahashi and D. L. Rousseau of AT&T Bell Laboratories for informing the authors of their data prior to publication. This study was supported by Grants-in-Aid of the Ministry of Education, Science, Culture, and Sports, Japan for Priority Areas (biometallics) to T.K. (08249106) and (cell energetics) to T.O. (04266105).

JA951922I

(49) Wikstrom, M. *Nature* **1989**, *338*, 776–778.